24th International Conference on Renewable Energies and Power Quality (ICREPQ'26)
Santander (Spain), 10th to 12th June 2026
ISBN-13: 978-84-09-82044-3

Receding Horizon Optimization of Residential Photovoltaic and Battery Storage Systems using Differential Evolution

J. Počivalnik[1], D. Kuhar[1], E. Simonič[1], B. Stergar[1], S. Seme[1,2] and K. Sredenšek[1,2]

[1] Faculty of Energy Technology, University of Maribor
Hočevarjev trg 1, 8270 Krško, Slovenia
e-mail: jernej.pocivalnik@um.si; domen.kuhar@um.si; eva.simonic@um.si; bojan.stergar@um.si; sebastijan.seme@um.si; klemen.sredensek@um.si

[2] Faculty of Electrical Engineering and Computer Science, University of Maribor
Koroška cesta 46, 2000 Maribor, Slovenia

Abstract.
The paper examines the use of receding horizon optimization combined with differential evolution for the control of a residential battery storage system integrated with a photovoltaic system. The objective is to reduce grid power peaks and overall electrical energy exchange with the grid by optimizing the operating strategy of the battery storage system. The proposed approach is evaluated using real household electrical energy consumption data and modeled photovoltaic system production with a 15-minute time resolution. Three receding horizon optimization configurations with different horizon lengths are analyzed under a fixed optimization time constraint. The results demonstrate that the performance of the battery storage system strongly depends on the selected optimization horizon. Moderate horizons provide a favorable compromise between look-ahead capability and convergence quality, while excessively long horizons suffer from limited convergence. The findings confirm that coordinated operation of photovoltaic and battery storage systems can improve local energy utilization and reduce stress on the electrical energy transmission and distribution system.

Key words.
Battery storage system, photovoltaic system, receding horizon optimization, differential evolution, grid interaction reduction

1. Introduction
Electrical energy transmission and distribution systems are undergoing significant changes due to increasing electrification of end-use sectors and the growing penetration of renewable energy sources. At the residential level, the deployment of electric vehicles and electric heating technologies has led to a substantial increase in electrical energy demand and peak loads. Analyses show that household electrification can result in peak power demands several times higher than current levels, posing serious challenges to existing power system infrastructure [1]. At the same time, the share of renewable energy sources, particularly photovoltaic (PV) systems, has been steadily increasing [2-4]. Despite their environmental benefits, renewable energy sources introduce additional operational challenges due to their intermittent and weather-dependent nature. The replacement of conventional synchronous generators with inverter-based sources has led to reduced system inertia and increased sensitivity to power imbalances, resulting in faster frequency dynamics [5-7]. In addition, the high penetration of distributed PV systems has raised concerns regarding voltage stability in distribution networks, where increased voltage fluctuations and component loading have been reported [8]. The growing number of prosumers further increases the complexity of power system operation. In this context, battery storage (BS) systems have become an important enabling technology, allowing surplus renewable energy to be stored and later utilized, thereby reducing grid stress and mitigating power fluctuations [9, 10]. Several analyses have also highlighted the role of BS systems in improving system flexibility and supporting stable operation in power systems with reduced inertia [11]. Recent research emphasizes that the benefits of BS systems depend strongly on the control strategy used. The charging and discharging decisions directly affect the state of charge and the amount of electrical energy exchanged with the grid, making control design a key factor for effective deployment [12, 13]. From a system perspective, properly controlled BS system can act as a source of flexibility, contributing to peak load reduction and improved integration of renewable energy production [14]. At the residential level, advanced control approaches, including optimization-based methods, have been proposed to address these challenges and enable more efficient local energy management [15].

This paper analyzes a household electricity consumer with an integrated PV system and BS system. The special importance and the main goal of the analysis is the optimal working principle of the BS system using differential evolution (DE). The analysis was based on electrical energy consumption data at 15-minute intervals, obtained from the Slovenian electrical energy consumption database, which is available for all users with digital electrical energy meters. Expected electrical energy production from the PV system was calculated using

annual solar radiation data from the Slovenian Environment Agency (ARSO), with values interpolated to 15-minute intervals to match the time resolution of the consumption data throughout the year. The calculation used an established model based on the fundamental astronomical relationships between the Sun and Earth [16].
For the considered optimization problem, DE was selected as the optimization method. DE is a stochastic population-based numerical optimization algorithm belonging to the class of evolutionary methods. It is mainly used to solve continuous optimization problems in which the objective function may be complex, nonlinear, or multimodal. One of the key strengths of DE is that it combines strong optimization performance with a straightforward algorithmic structure, making it easy to implement and efficient in practice. The algorithm improves a set of candidate solutions over multiple iterations by repeatedly generating new solutions from existing ones. This is achieved by using differences between randomly selected individuals in the population, which serve as a source of variation. Through this process, promising solutions are preserved while less effective ones are gradually replaced, allowing the population to move toward better regions of the search space without requiring problem-specific knowledge or gradient information [17-19]. In its simplest form, DE starts with a randomly generated population and iteratively applies mutation, crossover, and selection until a stopping condition is met. A flowchart of the main steps of the DE algorithm is shown in Fig. **Napaka! Vira sklicevanja ni bilo mogoče najti.**. Many analyses have shown that DE's behavior strongly depends on its control parameters and strategy choices, which has motivated extensive research on adaptive variants and theoretical properties. These developments have contributed to improved convergence reliability and a wider range of successful applications[17, 20, 21].

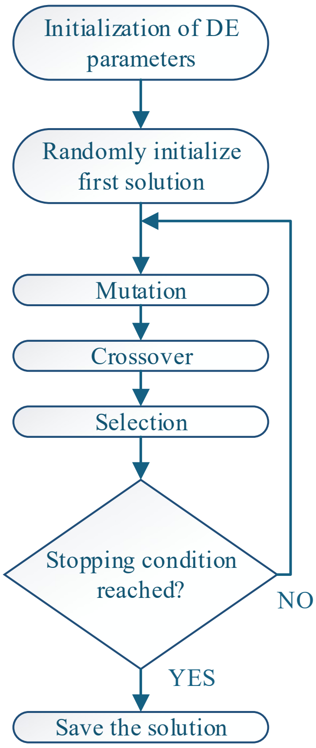

Fig. 1. DE algorithm.

2. Baseline state as input

The analysis was conducted on a small residential electrical energy consumer, namely a detached house located in the eastern part of Slovenia. Infrared (IR) panels were used for space heating, while a water boiler provided domestic hot water. The house was connected to the low voltage distribution grid through a 3×16 A fuse package. The measured electrical energy consumption data showed a relatively unbalanced load profile, primarily due to IR panels used for heating. The total annual electrical energy consumption amounted to 4,777 kWh, while the maximum recorded power demand was 4.82 kW. The complete annual electrical energy consumption profile is shown in Fig. 2 and represents the baseline operating state of the consumer, which was used as the input data for the subsequent optimization process.
For the purposes of this paper, the PV system was assumed to represent local electrical energy production at the household level. The PV system was selected to produce approximately 10% more electrical energy than the annual electrical energy consumption of the household. The assumed PV system consisted of eight BISOL BBO 450 PV modules, each with a nominal power of 450 W, resulting in a total installed nominal power of 3.6 kW. The estimated annual electrical energy production of the PV system was 5,345 kWh, while the maximum power reached 3.86 kW. The corresponding annual PV system production profile is presented in Fig. 3.

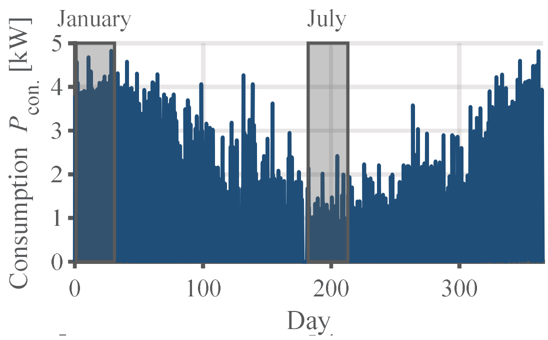

Fig. 2. Electrical energy consumption.

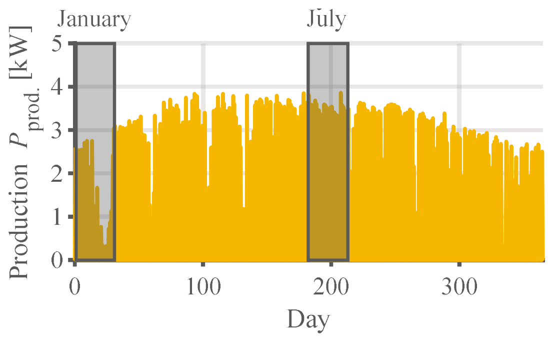

Fig. 3. PV system production.

Furthermore, two characteristic periods of the year, namely January and July, were highlighted in Fig. 2 and Fig. 3 by shaded gray areas. These months were deliberately selected due to their significantly different electrical energy consumption and production characteristics. January represented a winter operating scenario with increased electrical energy consumption from space heating and, simultaneously, reduced PV system electrical energy production due to unfavorable weather conditions and limited solar irradiation. In contrast, July represented a summer operating scenario with substantially lower household electrical energy consumption and considerably higher PV system electrical energy production, driven by longer daylight hours and higher solar irradiance. The pronounced contrast between these two periods provided a meaningful and challenging scenario for further analysis and optimization, as extreme operating conditions of both the consumer load and the PV system were captured.

3. Optimization framework

In addition to the baseline consumer and the assumed PV system, a BS system manufactured by SolarEdge was included in the analyzed system configuration. The BS system had a maximum energy capacity of 10 kWh. A depth of discharge of 97% was assumed, resulting in a minimum usable energy capacity of 0.3 kWh. The maximum charging and discharging power of the BS system was limited to 5 kW. These parameters defined the operational constraints of the BS system within the optimization framework.

The final objective, as stated previously, was to determine the optimal operating strategy of the BS system to minimize power peaks at the grid connection point in both directions. As a result, the obtained solution was also favorable in terms of the overall electrical energy interchange with the grid. To solve this optimization problem, DE was employed. The objective function of the DE was defined as the minimization of the sum of squared grid power values, as expressed in (1).

$$J(x) = \sum_{k=1}^{N} \left(P_{\text{grid}}\right)^2(k) \rightarrow 0 \qquad (1)$$

Where $J(x)$ denotes the objective function value to be minimized, x represents the vector of optimization variables describing the control actions of the BS system, k is the discrete time index, N is the total number of time steps within the considered optimization window, and $P_{\text{grid}}(k)$ is the power exchanged with the grid at time k. The quadratic formulation ensures that both positive and negative values of $P_{\text{grid}}(k)$ contribute positively to the objective function, thereby simultaneously penalizing grid power import and export and driving the overall grid power profile toward zero.

The optimization was performed with a discrete time step of 15 minutes (matching the consumption data resolution). Consequently, the length of the optimization horizon varied depending on the selected horizon duration. For a one day optimization horizon, the optimization window consisted of 96 time steps, while longer optimization horizons resulted in proportionally larger optimization windows, such as 192 time steps for a two-day optimization horizon and 384 time steps for a four-day optimization horizon. This approach enabled the investigation of different optimization horizons while maintaining a consistent temporal resolution.

Within this paper, three different receding horizon optimization configurations were considered. Receding-horizon optimization repeatedly solves an optimization problem over a finite horizon, with only a portion of the optimized control sequence implemented before the optimization is repeated with updated system states. In the first configuration, a one-day optimization horizon with a 12-hour implementation period was applied (1d12h). In the second configuration, a two-day optimization horizon with a one-day implementation period was used (2d1d). In the third configuration, a four-day optimization horizon with a two-day implementation period was adopted (4d2d). These configurations were selected in order to evaluate the influence of the optimization horizon length and the implementation period on the optimization results and the operating behavior of the BS system.

For all receding horizon optimization configurations, a fixed optimization time of 20 seconds per optimization horizon was imposed. This constraint was intentionally applied to ensure a fair comparison across configurations and to reflect realistic computational limitations. The fixed optimization time played a key role in the subsequent analysis, where the performance of individual configurations was compared with respect to both optimization quality and computational efficiency. In addition, all configurations employed the DE with consistent control parameters to ensure methodological uniformity. The crossover constant was set to CR = 0.5, and the mutation factor to F = 0.7. The selected mutation strategy was DE/rand-to-best/1/exp, enabling a balance between exploration and convergence speed. Furthermore, a value-to-reach criterion of VTR = 10^{-6} was used as an additional stopping condition.

4. Results

A. *Optimization results – January*

The operation of the BS system during January was characterized by increased household electrical energy consumption under winter operating conditions. The BS system power profiles for all considered receding horizon optimization configurations are shown in Fig. 4. Continuous charging and discharging actions were observed throughout the analyzed period, indicating that the BS system was actively utilized to modify the grid power profile in response to variations in household electrical energy consumption and PV system production.

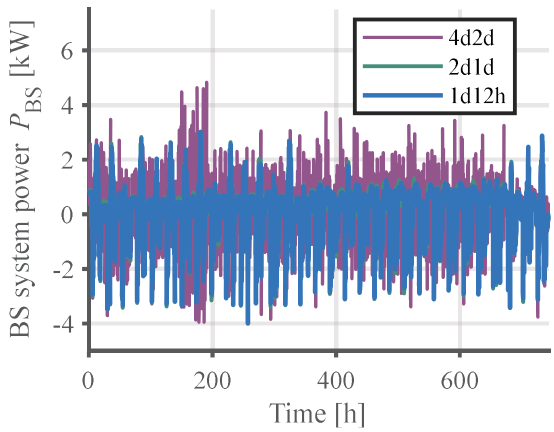

Fig. 4. BS system power.

The corresponding state of charge (SOC) profiles of the BS system for January are presented in Fig. 5. Frequent utilization of the available BS system energy capacity was observed, with repeated transitions between higher and lower SOC levels. The SOC remained within the predefined operational limits for all configurations, confirming that the imposed BS system constraints were respected within the optimization framework.

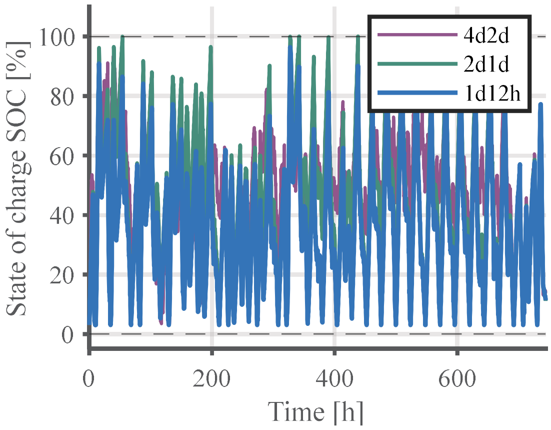

Fig. 5. BS system SOC.

The resulting grid interaction for January is illustrated in Fig. 6, where the optimized grid power profiles are shown together with the baseline household consumption profile. A visible modification in the grid power profile was observed during BS operation, with reduced grid power during periods of higher household electrical energy demand. The optimized grid power profiles were generally shifted closer to zero compared to the baseline consumption profile.

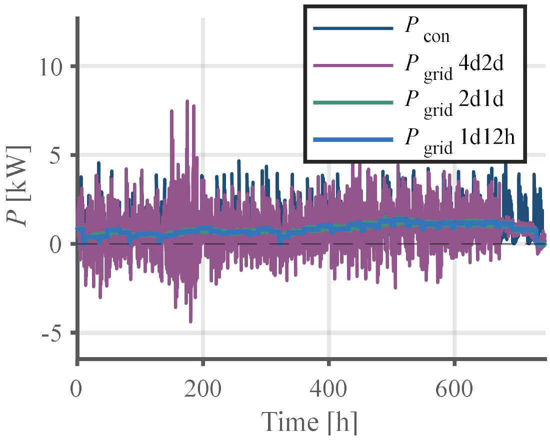

Fig. 6. Baseline consumption and optimized grid interaction.

The total exchanged electrical energy with the grid during January was also evaluated. In the baseline scenario without the BS system, a total of 719.06 kWh was exchanged, consisting of 662.79 kWh of electrical energy import and 56.27 kWh of electrical energy export. When the BS system was included, different levels of grid interaction were observed depending on the applied receding-horizon optimization configuration. For the 1d12h and 2d1d configurations, the total exchanged energy was reduced to approximately 607 kWh, corresponding to a reduction of about 15.5%. In contrast, for the 4d2d configuration, the total exchanged energy increased to 848.96 kWh, indicating greater overall grid interaction during winter operation.

B. *Optimization results – July*

The operation of the BS system during July was characterized by increased electrical energy production of the PV system and reduced household electrical energy consumption. The BS system power profiles for all receding-horizon optimization configurations are shown in Fig. 7. Frequent charging and discharging were observed throughout the analyzed period, reflecting active utilization of the BS system under summer operating conditions.

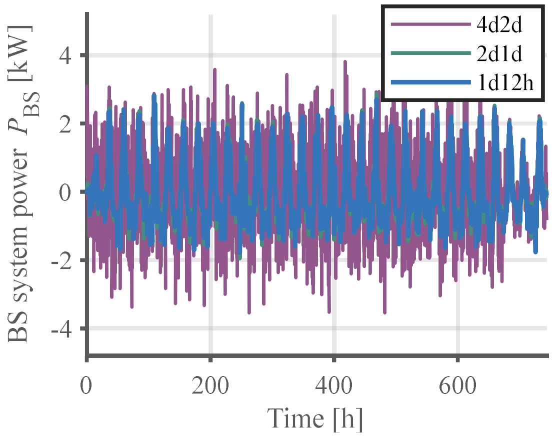

Fig. 7. BS system power.

The corresponding SOC profiles of the BS system for July are presented in Fig. 8. Higher average SOC levels were maintained compared to winter operation, with the SOC frequently approaching the upper operational limit. This behavior reflects the increased availability of locally produced electrical energy during the analyzed period.

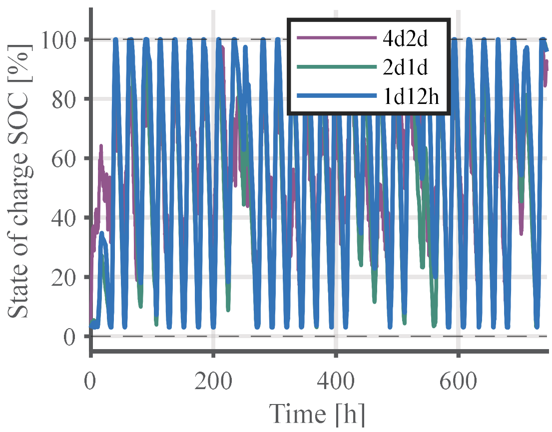

Fig. 8. BS system SOC.

The impact of the BS system on grid interaction in July is illustrated in Fig. 9, which shows the optimized grid power profiles alongside the baseline household consumption profile. A substantial modification of the grid power profile was observed, with a visible reduction in the magnitude of grid export. The optimized grid power profiles were significantly different from those in the baseline scenario without the BS system.

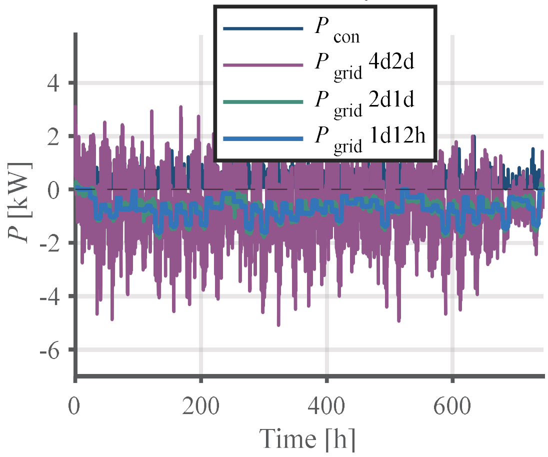

Fig. 9. Baseline consumption and optimized grid interaction.

The total exchanged electrical energy with the grid during July was also evaluated. In the baseline scenario without the BS system, the total exchanged energy amounted to 606.88 kWh, with electrical energy export accounting for 573.65 kWh. When the BS system was included, the total exchanged energy was reduced to approximately 532 kWh for the 1d12h and 2d1d configurations, corresponding to a reduction of about 12%. For the 4d2d configuration, the total exchanged energy increased to 853.15 kWh, indicating a substantial change in grid interaction under summer operating conditions.

5. Discussion

The presented results indicate that the performance of the BS system is strongly influenced by the selected receding-horizon optimization configuration when a fixed optimization time is imposed. In this paper, a constant optimization time of 20 s per optimization window was applied, enabling a direct assessment of convergence behavior and solution quality.

As the optimization horizon was extended from 1d12h to 4d2d, the number of decision variables increased significantly due to the fixed 15-minute time resolution. The resulting problem dimensionality amounted to 96, 192, and 384 discrete time steps for the 1d12h, 2d1d, and 4d2d configurations, respectively. Under a fixed optimization time constraint, this increase in dimensionality directly affected the convergence of the DE algorithm.

The accumulated optimization times further illustrate this effect. For January, total optimization times of 1,450.8 s, 873.3 s, and 306.4 s were recorded for the 1d12h, 2d1d, and 4d2d configurations, respectively. For July, similar values of 1,436.2 s, 828.6 s, and 303.8 s were obtained. These results indicate that shorter optimization horizons required a larger number of optimization windows, whereas longer horizons reduced the number of optimization calls while increasing the computational complexity of each individual optimization problem.

The convergence limitations of DE are clearly reflected in the number of iterations achieved per optimization window. For January, average iteration counts of 11,246, 4,243, and 1,444 were obtained for the 1d12h, 2d1d, and 4d2d configurations, respectively, while for July the corresponding values were 12,435, 4,345, and 1,514. The 4d2d configuration was therefore characterized by significantly reduced convergence capability due to the large number of decision variables and the increased computational cost per iteration.

As a result, the longest optimization horizon did not improve BS system performance and was associated with increased grid interaction in both analyzed months. In contrast, shorter and moderate optimization horizons enabled substantially better convergence within the imposed time limit.

The obtained results highlight a trade-off between time consumption and achievable solution quality. While longer optimization horizons theoretically provide greater foresight, their practical benefits are limited under strict computational constraints. Within the analyzed framework, the 2d1d configuration represented a balanced compromise, providing an extended look-ahead while maintaining sufficient convergence quality.

Seasonal operating conditions influenced the absolute levels of electrical energy import and export, with January characterized by higher electrical energy consumption and July by increased PV system production. However, similar convergence trends were observed in both months, indicating that the dominant limiting factor was computational feasibility rather than seasonal variability.

From a practical perspective, the results suggest that real-time BS system control strategies based on heuristic optimization should prioritize moderate optimization horizons and frequent reoptimization. Under realistic computational constraints, this approach provides more reliable, robust performance than excessively long optimization horizons.

6. Conclusion

The paper explores the use of receding horizon optimization combined with a differential evolution algorithm for the control of a BS system integrated with a PV system in a residential application. The proposed framework was evaluated using real consumption and PV system production data under winter and summer operating conditions, with the objective of reducing grid interaction. The results confirm that the operating strategy of the BS system has a decisive impact on its effectiveness. The contribution of the BS system to the reduction of grid dependency was shown to be strongly influenced by the selected optimization horizon, even when identical system parameters were applied. Under a fixed optimization time constraint, moderate optimization horizons performed better than longer ones, which were hampered by limited convergence. In particular, the two-day optimization horizon with daily implementation was identified as a practical compromise between time consumption and solution quality. The combined use of a PV system and a BS system was shown to represent a viable approach for improving local energy utilization, enhancing partial self-sufficiency, and reducing stress on the distribution grid. As a meaningful extension of this work, the incorporation of self-adaptive adjustment of differential evolution parameters is recommended, as it could further improve convergence behavior and yield better optimization results.

Acknowledgment

The authors acknowledge the use of research equipment DC power supply system for simulations of diffuse sources with an equipment set for managing energy systems together with a hybrid solar system, procured within the operation “Upgrading national research infrastructures – RIUM”, which was co-financed by the Republic of Slovenia and the European Union from the European Regional Development Fund.

References

[1] Priyadarshan, C. Crozier, K. Baker, and K. J. Kircher, “Distribution grids may be a barrier to residential electrification,” *Cell Reports Sustainability,* vol. 2, no. 11, Nov 21, 2025.

[2] M. Basílio, “Renewable energy and energy efficiency: An exploratory study in EU countries,” *Sustainable Futures,* vol. 9, Jun, 2025.

[3] G. Di Foggia, and M. Beccarello, “European roadmaps to achieving 2030 renewable energy targets,” *Utilities Policy,* vol. 88, Jun, 2024.

[4] R. Puertas, and L. Marti, “Renewable energy production capacity and consumption in Europe br,” *Science of the Total Environment,* vol. 853, Dec 20, 2022.

[5] S. Lim, T. Kim, K. Y. Lee, D. Choi, and J. W. Park, “Impact of high penetration of renewables on power system frequency response: A review and verification,” *Renewable & Sustainable Energy Reviews,* vol. 217, Jul, 2025.

[6] S. Saha, M. I. Saleem, and T. K. Roy, “Impact of high penetration of renewable energy sources on grid frequency behaviour,” *International Journal of Electrical Power & Energy Systems,* vol. 145, Feb, 2023.

[7] A. M. Saleh, I. Vokony, M. Waseem, M. A. Khan, and A. Al-Areqi, “Power system stability with high integration of RESs and EVs: Benefits, challenges, tools, and solutions,” *Energy Reports,* vol. 13, pp. 2637–2663, Jun, 2025.

[8] N. Damianakis, G. R. C. Mouli, and P. Bauer, “Grid impact of photovoltaics, electric vehicles and heat pumps on distribution grids - An overview,” *Applied Energy,* vol. 380, Feb 15, 2025.

[9] A. A. K. Arani, G. B. Gharehpetian, and M. Abedi, “Review on Energy Storage Systems Control Methods in Microgrids,” *International Journal of Electrical Power & Energy Systems,* vol. 107, pp. 745–757, May, 2019.

[10] F. H. Malik, G. A. Hussain, Y. M. S. Alsmadi, Z. M. Haider, W. Mansoor, and M. Lehtonen, “Integrating Energy Storage Technologies with Renewable Energy Sources: A Pathway Toward Sustainable Power Grids,” *Sustainability,* vol. 17, no. 9, May 1, 2025.

[11] C. Y. Zhao, P. B. Andersen, C. Traeholt, and S. Hashemi, “Grid-connected battery energy storage system: a review on application and integration,” *Renewable & Sustainable Energy Reviews,* vol. 182, Aug, 2023.

[12] N. G. Chatzigeorgiou, S. Theocharides, G. Makrides, and G. E. Georghiou, “A review on battery energy storage systems: Applications, developments, and research trends of hybrid installations in the end-user sector,” *Journal of Energy Storage,* vol. 86, May 1, 2024.

[13] E. O'Shaughnessy, D. Cutler, K. Ardani, and R. Margolis, “Solar plus: Optimization of distributed solar PV through battery storage and dispatchable load in residential buildings,” *Applied Energy,* vol. 213, pp. 11–21, Mar 1, 2018.

[14] T. Ferrucci, D. Fioriti, D. Poli, S. Barberis, F. Roncallo, and V. Gambino, “Battery energy storage systems for ancillary services in renewable energy communities,” *Applied Thermal Engineering,* vol. 260, Feb 1, 2025.

[15] A. C. Real, G. P. Luz, J. M. C. Sousa, M. C. Brito, and S. M. Vieira, “Optimization of a photovoltaic-battery system using deep reinforcement learning and load forecasting,” *Energy and Ai,* vol. 16, May, 2024.

[16] S. Seme, K. Sredensek, B. Stumberger, and M. Hadziselimovic, “Analysis of the performance of photovoltaic systems in Slovenia,” *Solar Energy,* vol. 180, pp. 550–558, Mar 1, 2019.

[17] S. Das, and P. N. Suganthan, “Differential Evolution: A Survey of the State-of-the-Art,” *Ieee Transactions on Evolutionary Computation,* vol. 15, no. 1, pp. 4–31, Feb, 2011.

[18] T. Eltaeib, and A. Mahmood, “Differential Evolution: A Survey and Analysis,” *Applied Sciences-Basel,* vol. 8, no. 10, Oct, 2018.

[19] R. Storn, and K. Price, “Differential evolution - A simple and efficient heuristic for global optimization over continuous spaces,” *Journal of Global Optimization,* vol. 11, no. 4, pp. 341–359, Dec, 1997.

[20] S. Das, S. S. Mullick, and P. N. Suganthan, “Recent advances in differential evolution - An updated survey,” *Swarm and Evolutionary Computation,* vol. 27, pp. 1–30, Apr, 2016.

[21] K. R. Opara, and J. Arabas, “Differential Evolution: A survey of theoretical analyses,” *Swarm and Evolutionary Computation,* vol. 44, pp. 546–558, Feb, 2019.